NFN - Nationales Forschungsnetzwerk

Geometry + Simulation

http://www.gs.jku.at

Isogeometric Analysis with Geometrically Continuous Functions

M. Kapl, V. Vitrih, B. Jüttler,

G+S Report No. 22

December 2014

Der Wissenschaftsfonds.

JOHANNES KEPLER UNIVERSITY LINZ

Isogeometric Analysis with Geometrically Continuous Functions

Mario Kapl[a], Vito Vitrih[b], Bert Jüttler[a,*]

[a]*Institute of Applied Geometry, Johannes Kepler University, Linz, Austria*
[b]*IAM and FAMNIT, University of Primorska, Koper, Slovenia*

Abstract

We study the linear space of C^s-smooth isogeometric functions defined on a multi-patch domain $\Omega \subset \mathbb{R}^2$. We show that the construction of these functions is closely related to the concept of geometric continuity of surfaces, which has originated in geometric design. More precisely, the C^s-smoothness of isogeometric functions is found to be equivalent to geometric smoothness of the same order (G^s-smoothness) of their graph surfaces. This motivates us to call them C^s-smooth geometrically continuous isogeometric functions. We present a general framework to construct a basis and explore potential applications in isogeometric analysis. Numerical experiments with bicubic and biquartic functions for performing L^2 approximation and for solving Poisson's equation and the biharmonic equation on two-patch geometries are presented and indicate optimal rates of convergence.

Keywords: Isogeometric Analysis, geometric continuity, geometrically continuous isogeometric functions, biharmonic equation, multi-patch domain
2000 MSC: 65D17, 65N30, 68U07

1. Introduction

In the framework of Isogeometric Analysis (IgA), which was introduced in [8], partial differential equations are discretized by using functions that are obtained from a parameterization of the computational domain. Typically one considers parameterizations by polynomial or rational spline functions (NURBS – non-uniform rational spline functions, see [16]) but other types of functions have been used also. On the one hand, this approach facilitates the data exchange with geometric design tools, since the mathematical technology used in Computer Aided Design (CAD) is based on parametric representations of curves and surfaces. On the other hand, it has been observed that the increased smoothness of the spline functions compared to traditional finite elements has a beneficial effect on stability and convergence properties [3, 6].

Clearly, regular single-patch NURBS parameterizations are available only for domains that are topologically equivalent to a box. Though it is possible to extend the applicability of such parameterizations slightly by considering parameterizations with singular points

*Corresponding author
Email addresses: `mario.kapl@jku.at` (Mario Kapl), `vito.vitrih@upr.si` (Vito Vitrih), `bert.juettler@jku.at` (Bert Jüttler)

(cf. [23]), it is preferable to use other techniques, due to the difficulties introduced by the use of singularities.

One of the most promising approaches is to use multi-patch parameterizations, which are coupled across their interfaces. Several coupling techniques are available, such as the direct identification of the degrees of freedom along the boundaries as in [20], the use of Lagrangian multipliers as in [10], or Nitsche's method [12]. The approximation power of T-spline representations of two-patch geometries was explored in [2]. However, these multi-patch constructions in isogeometric analysis are limited to functions of low regularity (at most C^0 smoothness). Consequently, the resulting numerical solutions are highly smooth almost everywhere, except across the interfaces between the patches of the multi-patch discretization.

Another approach is the use of trimmed NURBS geometries, which can also be combined with the multi-patch method. Such geometries have been used in the context of IgA (see e.g. [9, 17, 19]). However, trimming implies unavoidable gaps, when two trimmed NURBS patches are joined together (cf. [21]), and often requires advanced techniques for coupling the discretizations, see [17]. Another related technique is the use of mapped B-splines on general meshes [24].

The use of functions generated by subdivision algorithms has become a valuable alternative to NURBS, especially in Computer Graphics, since these functions lead to gap-free surfaces of arbitrary topology (cf. [15]). One of the standard subdivision methods is the Catmull-Clark subdivision, which generates surfaces consisting of bicubic patches, joined with C^2-smoothness everywhere except at extraordinary vertices, where they have a well-defined tangent plane. A Catmull-Clark based isogeometric method for solids is presented in [4]. Disadvantages of using subdivision methods are the possible reduction of the approximation power in the vicinity of extraordinary vertices, cf. [11] and the need for special numerical integration techniques. In fact these functions are piecewise polynomial functions with an infinite number of segments.

Another possibility to deal with domains of general topology is the use of T-splines, which are a generalization of NURBS that allow T-junctions and extraordinary vertices in the mesh (cf. [22]). Consequently, T-meshes can represent more complex geometries, and this has been exploited in IgA, see e.g. [1, 2]. However, the mathematical properties of the resulting isogeometric functions around the extraordinary vertices are not well understood. Around extraordinary vertices, T-splines are based on a special construction for geometrically continuous surfaces.

Geometric continuity is a well-known and highly useful concept in geometric design [13] and there exist numerous constructions for multi-patch surfaces with this property. It can be used to construct isogeometric functions of higher smoothness [14], but the systematic exploration of the potential for IgA has just started. Numerical experiments with a multi-patch parameterization of a disk have been presented in [11]. The results indicate again a reduction of the approximation power (and consequently a lower order of convergence) which is caused by the extraordinary vertices, similar to the case of subdivision algorithms.

Our paper consists of two main parts. In the first part, which consists of Sections 2 and 3, we describe the concept of geometrically continuous isogeometric functions on general multi-patch domains, and we present a framework for computing a basis of the corresponding isogeometric discretization space. In the second part (Section 4), we investigate the approximation power of geometrically continuous isogeometric functions for a specific configuration of two-patch geometries, in order to demonstrate their potential for IgA. In addition to L^2 approximation and solving Poisson's equation, we also present results concerning the biharmonic equation, where the use of C^1-smooth test functions greatly facilitates the (isogeometric) discretization. Our numerical results indicate that the geometrically continuous representations maintain the full approximation power. This may be due to the fact that the effect of geometric continuity in our approach is not restricted to the vicinity of an extraordinary vertex as in earlier approaches, but spread out along the entire interface between the patches.

2. Geometrically continuous isogeometric functions

In order to simplify the presentation we restrict ourselves to the case of two-dimensional computational domains. Given a positive integer n, we consider n bijective, regular geometry mappings

$$\boldsymbol{G}^{(\ell)} : [0,1]^2 \to \mathbb{R}^2, \quad \ell \in \{1, \ldots n\},$$

which are represented in coordinates by

$$\boldsymbol{\xi}^{(\ell)} = (\xi_1^{(\ell)}, \xi_2^{(\ell)}) \mapsto (G_1^{(\ell)}, G_2^{(\ell)}) = \boldsymbol{G}^{(\ell)}(\boldsymbol{\xi}^{(\ell)}),$$

with $\boldsymbol{G}^{(\ell)} \in \mathcal{S}^{(\ell)}$, where $\mathcal{S}^{(\ell)}$ is a tensor-product NURBS space of degree $d_\ell \in \mathbb{N}_0^2$. Consequently, each geometry mapping $\boldsymbol{G}^{(\ell)}$, $\ell \in \{1, \ldots, n\}$, is defined as a linear combination of NURBS basis functions $\psi_{\boldsymbol{i}}^{(\ell)} : [0,1]^2 \to \mathbb{R}$, i.e.,

$$\boldsymbol{G}^{(\ell)}(\boldsymbol{\xi}^{(\ell)}) = \sum_{\boldsymbol{i} \in I_\ell} \boldsymbol{d}_{\boldsymbol{i}}^{(\ell)} \psi_{\boldsymbol{i}}^{(\ell)}(\boldsymbol{\xi}^{(\ell)}),$$

with a suitable index set I_ℓ (a box in index space) and control points $\boldsymbol{d}_{\boldsymbol{i}}^{(\ell)} \in \mathbb{R}^2$. Thus it is a two-dimensional regular NURBS surface patch in $\mathbb{R}^2$. Each geometry mapping $\boldsymbol{G}^{(\ell)}$, $\ell \in \{1, \ldots, n\}$, defines a quadrilateral subdomain or patch

$$\Omega^{(\ell)} = \boldsymbol{G}^{(\ell)}([0,1]^2).$$

We assume that the interiors of these subdomains are mutually disjoint, i.e.

$$\boldsymbol{G}^{(\ell)}((0,1)^2) \cap \boldsymbol{G}^{(k)}((0,1)^2) = \emptyset$$

for $\ell, k \in \{1, \ldots, n\}$ with $\ell \neq k$. The computational domain $\Omega \subset \mathbb{R}^2$ is the union of these quadrilateral patches $\Omega^{(\ell)}$, i.e.,

$$\Omega = \bigcup_{\ell=1}^{n} \Omega^{(\ell)}.$$

On each patch $\Omega^{(\ell)}$, $\ell \in \{1, \ldots, n\}$, the space of isogeometric functions is given by

$$\mathcal{S}^{(\ell)} \circ (\boldsymbol{G}^{(\ell)})^{-1}.$$

Given a positive integer s, which specifies the order of smoothness, the space

$$V = \left\{ v \in C^s(\Omega) : v|_{\Omega^{(\ell)}} \in \mathcal{S}^{(\ell)} \circ (\boldsymbol{G}^{(\ell)})^{-1} \text{ for all } \ell \in \{1, \ldots, n\} \right\}$$

contains the *globally C^s-smooth isogeometric functions* defined on the computational domain Ω.

Let us consider an isogeometric function $w \in V$ in more detail. On each patch $\Omega^{(\ell)}$, $\ell \in \{1, \ldots, n\}$, the function w is represented by

$$(w|_{\Omega^{(\ell)}})(\boldsymbol{x}) = w^{(\ell)}(\boldsymbol{x}) = \left(\omega^{(\ell)} \circ (\boldsymbol{G}^{(\ell)})^{-1} \right)(\boldsymbol{x}), \quad \boldsymbol{x} \in \Omega^{(\ell)}, \tag{1}$$

with $\omega^{(\ell)} \in \mathcal{S}^{(\ell)}$. Note the difference between $\omega^{(\ell)}$, which is a function defined on the local parameter domain $[0,1]^2$, and $w^{(\ell)}$, which is the associated segment of the isogeometric function defined on $\Omega^{(\ell)}$.

The associated graph surface $\boldsymbol{F}^{(\ell)}$ of $w^{(\ell)}$ possesses the form

$$\boldsymbol{F}^{(\ell)}(\boldsymbol{\xi}^{(\ell)}) = \Big(\underbrace{G_1^{(\ell)}(\boldsymbol{\xi}^{(\ell)}), G_2^{(\ell)}(\boldsymbol{\xi}^{(\ell)})}_{=\boldsymbol{G}^{(\ell)}(\boldsymbol{\xi}^{(\ell)})}, \omega^{(\ell)}(\boldsymbol{\xi}^{(\ell)}) \Big)^T.$$

For any bivariate function f we denote with $\partial_i f$ its partial derivative with respect to the i-th argument. Depending on the domain of the function, this argument can be either one of the local parameters $\xi_i^{(\ell)}$ or one of the coordinates x_i in the physical domain.

We consider two neighboring patches $\Omega^{(\ell)}$ and $\Omega^{(k)}$ with the common interface $\boldsymbol{e}^{(\ell k)} = \Omega^{(\ell)} \cap \Omega^{(k)}$, see Figure 1. Since $w \in C^s(\Omega)$, the derivatives up to order s of the functions $w^{(\ell)}$ and $w^{(k)}$ at the common interface have to be equal, i.e.,

$$(\partial_1^i \partial_2^j w^{(\ell)})(\boldsymbol{x}) = (\partial_1^i \partial_2^j w^{(k)})(\boldsymbol{x}), \quad \boldsymbol{x} \in \boldsymbol{e}^{(\ell k)}, \tag{2}$$

for $i + j \leq s$, where $\boldsymbol{x} = (x_1, x_2)$ are the global (world) coordinates with respect to the computational domain Ω. We evaluate the derivatives at the boundary of the patches by considering one-sided limits. Moreover we assume that the geometry mappings and their inverses are at least C^s smooth.

We can also parameterize the graph surfaces $\boldsymbol{F}^{(\ell)}$ and $\boldsymbol{F}^{(k)}$ with respect to the world coordinates x_1 and x_2, simply as

$$\left(x_1, x_2, w^{(\ell)}(x_1, x_2)\right)^T \text{ and } \left(x_1, x_2, w^{(k)}(x_1, x_2)\right)^T.$$

Clearly, these two parameterized surfaces are joined together with C^s smoothness along $\boldsymbol{e}^{(\ell k)}$. This is obvious for the first two coordinates, and it is implied by (2) for the third one. Recall that two parametric surfaces are said to be joined together with *geometric smoothness of order s* if there exist reparameterizations (parameter transformations) that

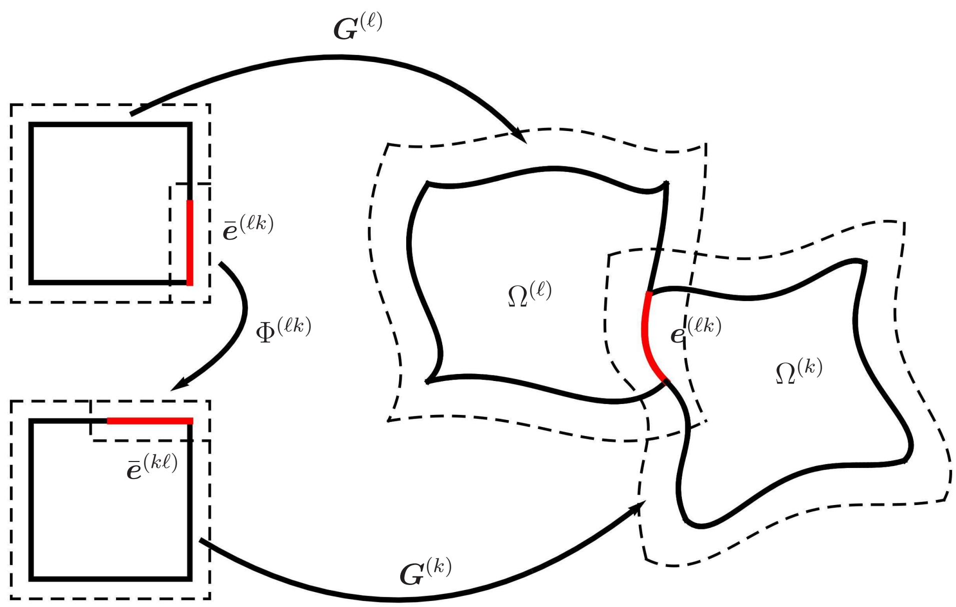

Figure 1: The geometry mappings $\boldsymbol{G}^{(\ell)}$ and $\boldsymbol{G}^{(k)}$ which are defined on a neighborhood of $[0,1]^2$.

transform them into two parametric surfaces that are joined together with C^s smoothness [7, 13]. (Typically only a reparameterization of one of the two surfaces is considered, but it is also possible to reparameterize both surfaces.) The two graph surfaces $\boldsymbol{F}^{(\ell)}$ and $\boldsymbol{F}^{(k)}$ satisfy the criterion of this definition. We thus obtain:

Theorem 1. *Let $w : \Omega \to \mathbb{R}$ be an isogeometric function, which is defined on patches $\Omega^{(\ell)}$, $\ell \in \{1, \ldots, n\}$, by isogeometric functions $w^{(\ell)}$, given in* (1)*. Then $w \in V$ if and only if for all neighboring patches $\Omega^{(\ell)}$ and $\Omega^{(k)}$, $\ell, k \in \{1, \ldots, n\}$ with $\ell \neq k$, the associated graph surfaces $\boldsymbol{F}^{(\ell)}$ and $\boldsymbol{F}^{(k)}$ meet at the common interface with geometric continuity of order s.*

Consequently, we will refer to the functions $w \in V$ as C^s*-smooth geometrically continuous isogeometric functions*. In fact, the surfaces themselves possess the standard smoothness properties, but their graph surfaces are joined with geometric continuity.

The conditions (2) are equivalent to

$$(\partial_1^i \partial_2^j \omega^{(\ell)})(\boldsymbol{\xi}^{(\ell)}) = (\partial_1^i \partial_2^j (\omega^{(k)} \circ \underbrace{\left(\boldsymbol{G}^{(k)}\right)^{-1} \circ \boldsymbol{G}^{(\ell)}}_{=\boldsymbol{\phi}^{(\ell k)}}))(\boldsymbol{\xi}^{(\ell)}), \quad \boldsymbol{\xi}^{(\ell)} \in \bar{\boldsymbol{e}}^{(\ell k)}, \tag{3}$$

for $i+j \leq s$, where $\bar{\boldsymbol{e}}^{(\ell k)} = \left(\boldsymbol{G}^{(\ell)}\right)^{-1}(\boldsymbol{e}^{(\ell k)})$. To make these conditions well-defined, we additionally assume that the geometry mappings $\boldsymbol{G}^{(\ell)}$ and $\boldsymbol{G}^{(k)}$ are defined on a neighborhood of $[0,1]^2$, and that the reparameterization

$$\boldsymbol{\phi}^{(\ell k)} : [0,1]^2 \to [0,1]^2 : \quad \boldsymbol{\phi}^{(\ell k)}(\boldsymbol{\xi}^{(\ell)}) = \left((\boldsymbol{G}^{(k)})^{-1} \circ \boldsymbol{G}^{(\ell)}\right)(\boldsymbol{\xi}^{(\ell)})$$

is hence also defined on the neighborhood of $\bar{\boldsymbol{e}}^{(\ell k)}$ (see Figure 1).

Note that the conditions (3) are automatically satisfied for the functions

$$\omega^{(\ell)} = G_1^{(\ell)}, \quad \omega^{(k)} = G_1^{(k)}$$

and

$$\omega^{(\ell)} = G_2^{(\ell)}, \quad \omega^{(k)} = G_2^{(k)}.$$

Returning to the general case and using these two observations, we conclude that the graphs $\boldsymbol{F}^{(\ell)}$ and $\boldsymbol{F}^{(k)}$ in (3) fulfill the conditions

$$(\partial_1^i \partial_2^j \boldsymbol{F}^{(\ell)})(\boldsymbol{\xi}^{(\ell)}) = (\partial_1^i \partial_2^j (\boldsymbol{F}^{(k)} \circ \boldsymbol{\phi}^{(\ell k)}))(\boldsymbol{\xi}^{(\ell)}), \quad \boldsymbol{\xi}^{(\ell)} \in \bar{\boldsymbol{e}}^{(\ell k)}, \tag{4}$$

for $i+j \leq s$, which is again in agreement with the definition of geometric continuity between two surface patches. Consequently, Theorem 1 is equivalent to a very recent result of Peters [14], who observed that *matched G^1-constructions yield C^1-continuous isogeometric elements*, and to the possible extension of that result to higher order smoothness.

In contrast to the approach in [14], which is based on the usual viewpoint in geometric design, we started our derivation from the given domain parameterization and not from the reparameterization $\boldsymbol{\phi}^{(\ell k)}$. We feel that this viewpoint fits better into the IGA framework, where the computational domain is central. It also leads to a natural framework for the construction of a basis of the space V. This is described in the next section.

3. Constructing a basis for geometrically continuous isogeometric functions

Constructing a basis is an essential first step, which is required in order to use geometrically continuous isogeometric functions for simulations. We will construct isogeometric basis functions on Ω, which span the space V of all C^s smooth geometrically continuous isogeometric functions. On each patch $\Omega^{(\ell)}$, $\ell \in \{1, 2, \ldots n\}$, any such basis function – which we again denote by w – is given by a representation of the form (1). According to Theorem 1, the functions w are C^s–smooth on Ω if and only if the graph surfaces join with geometric smoothness of order s across the common interface $\boldsymbol{e}^{(\ell k)}$ for all neighboring patches $\Omega^{(\ell)}$, $\Omega^{(k)}$, $\ell, k \in \{1, 2, \ldots, n\}$, with $\ell \neq k$.

We choose a basis $(\psi_{\boldsymbol{j}}^{(\ell)})_{\boldsymbol{j} \in I_\ell}$ for each local spline space $\mathcal{S}^{(\ell)}$, e.g., the NURBS basis functions on each patch. Consequently, the functions $\omega^{(\ell)} \in \mathcal{S}^{(\ell)}$, which define the basis function, have a local representations

$$\omega^{(\ell)}(\boldsymbol{\xi}^{(\ell)}) = \sum_{\boldsymbol{j} \in I_\ell} b_{\boldsymbol{j}}^{(\ell)} \psi_{\boldsymbol{j}}^{(\ell)}(\boldsymbol{\xi}^{(\ell)}).$$

Using Eq. (1) and (2) we obtain constraints on their coefficients,

$$\sum_{\boldsymbol{j} \in I_\ell} b_{\boldsymbol{j}}^{(\ell)} (\partial_1^i \partial_2^j (\psi_{\boldsymbol{j}}^{(\ell)} \circ \left(\boldsymbol{G}^{(\ell)}\right)^{-1}))(\boldsymbol{x}) = \sum_{\boldsymbol{j} \in I_k} b_{\boldsymbol{j}}^{(k)} (\partial_1^i \partial_2^j (\psi_{\boldsymbol{j}}^{(k)} \circ \left(\boldsymbol{G}^{(k)}\right)^{-1}))(\boldsymbol{x}), \quad \boldsymbol{x} \in \boldsymbol{e}^{(\ell k)}, \tag{5}$$

Since we are considering a finite-dimensional space of functions, these constraints are equivalent to finitely many linear constraints on the coefficients $b_{\boldsymbol{j}}^{(\ell)}$ and $b_{\boldsymbol{j}}^{(k)}$, which can be formulated as a homogeneous linear system

$$S\boldsymbol{b} = 0, \quad \boldsymbol{b} = \left(b_{\boldsymbol{j}}^{(\ell)}\right)_{\boldsymbol{j}\in I_\ell, \ell\in\{1,2,\ldots,n\}}. \tag{6}$$

We may choose a basis of the null space (the kernel) of the matrix S. Each basis vector defines now via (1) a function

$$\omega_i = \left(\omega_i^{(\ell)}\right)_{\ell\in\{1,2,\ldots,n\}}, \ i = 1, 2, \ldots, \dim(\ker S).$$

Consequently, every function ω_i then defines by (1) an isogeometric basis function

$$w_i = \left(w_i^{(\ell)}\right)_{\ell\in\{1,2,\ldots,n\}} \in C^s(\Omega).$$

Clearly, a possible strategy for a suitable basis of the null space of S could be the selection of local basis functions with small supports and the avoidance of (global) basis functions having large supports if feasible. Moreover, it is possible to extend the linear system (6) by adding further linear equations to satisfy certain conditions for the basis, e.g., the fulfillment of the boundary conditions for solving the Poisson's equation and the biharmonic equation (see Sections 4.3 and 4.4).

Let us consider the case of two patches for $s = 1$ in more detail.

Example 2. We consider two patches $\boldsymbol{G}^{(\ell)}(\boldsymbol{\xi}^{(\ell)})$ and $\boldsymbol{G}^{(k)}(\boldsymbol{\xi}^{(k})$ with a common edge,

$$\boldsymbol{G}^{(\ell)}(1, \xi_2) = \boldsymbol{G}^{(k)}(0, \xi_2), \quad \xi_2 = \xi_2^{(\ell)} = \xi_2^{(k)} \in [0, 1], \tag{7}$$

which is parameterized identically by both NURBS patches. Consequently, the isogeometric function is continuous across this edge if

$$\omega^{(\ell)}(1, \xi_2) = \omega^{(k)}(0, \xi_2). \tag{8}$$

We consider the tangent planes of the two graph surfaces $\boldsymbol{F}^{(\ell)}$ and $\boldsymbol{F}^{(k)}$ at the points of the common edge. They are spanned by the derivative vectors

$$\partial_1\boldsymbol{F}^{(\ell)}(1, \xi_2),\ \partial_2\boldsymbol{F}^{(\ell)}(1, \xi_2) \text{ and } \partial_1\boldsymbol{F}^{(k)}(0, \xi_2),\ \partial_2\boldsymbol{F}^{(k)}(0, \xi_2),$$

respectively. The C^1-smoothness of the isogeometric test function is guaranteed if the 3×4 matrix formed by them has rank 2 only, since then the two tangent planes at any point $\boldsymbol{G}^{(\ell)}(1, \xi_2)$ are identical. Due to the identity

$$\partial_2\boldsymbol{F}^{(\ell)}(1, \xi_2) = \partial_2\boldsymbol{F}^{(k)}(0, \xi_2),$$

which is implied by the continuity conditions (7) and (8), this is equivalent to

$$\det\Big((\partial_1\boldsymbol{F}^{(\ell)})(1, \xi_2), (\partial_1\boldsymbol{F}^{(k)})(0, \xi_2), (\partial_2\boldsymbol{F}^{(k)})(0, \xi_2)\Big) = 0, \quad \xi_2 \in [0, 1], \tag{9}$$

which is a well-known condition for first oder geometric continuity between two surface patches, cf. [7]. If for example $\boldsymbol{F}^{(\ell)}$ and $\boldsymbol{F}^{(k)}$ are polynomial patches, then the left-hand side of (9) is a polynomial and we can obtain the desired system of linear equations (6) by setting all its coefficients to zero. $\Diamond$

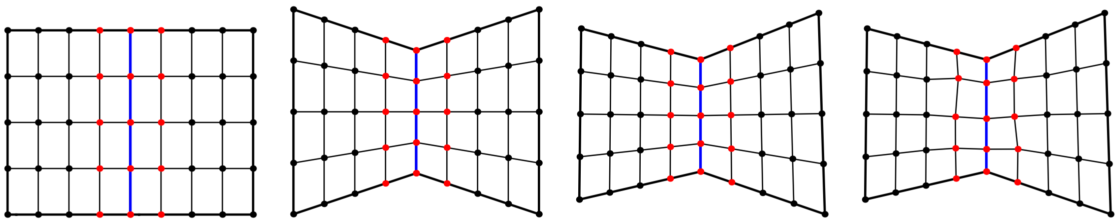

(a) (b) (c) (d)

Figure 2: Different two-patch domains which are defined by two biquartic Bézier patches $\boldsymbol{G}^{(1)}$ and $\boldsymbol{G}^{(2)}$. The blue edge is the common edge of both patches. Only the red control points influence the dimension. The black ones can be chosen arbitrarily.

k	Domain (a)	Domain (b)	Domain (c)	Domain (d)
0	10	10	9	3
1	16	16	13	3
2	22	21	17	3
3	28	26	21	3
$k \geq 1$ (conjecture)	$10 + 6k$	$11 + 5k$	$9 + 4k$	3

Table 1: The number of geometrically continuous isogeometric basis functions of the second type for some particular values of k for the domains shown in Fig. 2. For general k, the number is conjectured.

The dimension of the null space of S depends heavily on the geometry. The following example for different two-patch domains demonstrates this observation.

Example 3. Let us consider four different pairs of geometry mappings $\boldsymbol{G}^{(1)}$ and $\boldsymbol{G}^{(2)}$, which define computational domains Ω consisting of two quadrilateral patches $\Omega^{(1)}$ and $\Omega^{(2)}$ (see Figure 2). All initial geometry mappings are given as biquartic Bézier patches $[0,1]^2 \to \mathbb{R}^2$. For the instances (a)-(c), these patches are (suitably degree-elevated) bilinear representations of the plane, whereas in (d), the two patches are non-degenerate biquartic representations, which are obtained by slightly changing the red control points of the biquartic Bézier patches of (c), except the points on the boundary of the domain Ω. In addition, the domains (a) and (b) consist of two symmetric rectangles and trapezoids, respectively, which is in contrast to the domains (c) and (d), where the two patches are not symmetric.

It should be noted that the results presented below concerning the dimension of V depend only on the location of the control points along the interface and in the two neighboring columns, which are shown in red. The location of the remaining control points can be modified.

By inserting in both parameter directions $k \in \mathbb{N}_0$ equidistant inner knots of multiplicity 3, we arrive at the knot vectors

$$(0,0,0,0,0,\tfrac{1}{k+1},\tfrac{1}{k+1},\tfrac{1}{k+1},\tfrac{2}{k+1},\tfrac{2}{k+1},\tfrac{2}{k+1},\ldots,\tfrac{k}{k+1},\tfrac{k}{k+1},\tfrac{k}{k+1},1,1,1,1,1),$$

and obtain a B-spline representation of degree $(4,4)$ of the biquartic Bézier patches $\boldsymbol{G}^{(1)}$ and $\boldsymbol{G}^{(2)}$. For each pair of these B-spline representations, it is possible to construct two different kinds of C^1-smooth geometrically continuous isogeometric functions, which contribute to a basis of the space V.

The *basis functions of the first kind* consists of local basis functions with a support that is contained in one of the two patches only. More precisely, these functions are obtained by composing the biquartic tensor-product B-splines on one of the patches with the inverse geometry mappings,

$$\psi_{\boldsymbol{i}}^{(\ell)} \circ (\boldsymbol{G}^{(\ell)})^{-1}$$

where the support of the B-spline does not intersect the interface with the other patch. Consequently, these functions have only one non-zero coefficient $b_{\boldsymbol{j}}^{(\ell)}$ and all coefficients $b_{\boldsymbol{j},i}^{(\ell)}$ of these functions, which correspond to the control points of the common edge or one of the neighboring columns of the two patches $\boldsymbol{G}^{(1)}$ and $\boldsymbol{G}^{(2)}$ (i.e the red control points for $k = 0$), are zero. Since the coefficients $b_{\boldsymbol{j},i}^{(\ell)}$ of these isogeometric functions do not depend on the initial geometry, they have the same value for all four instances (a)-(d), and we obtain the same number of such functions for all cases.

In contrast, the *functions of the second kind* depend on the initial geometry. Here, the coefficients $b_{\boldsymbol{j},i}^{(\ell)}$, which do not correspond to the control points of the common edge or one of the neighboring columns of the two resulting spline patches, are zero.

Let $\nu(k)$ denote the number of the functions of the second kind, which are obtained by inserting in both parameter directions $k \geq 0$ equidistant inner knots of multiplicity 3. This number heavily depends on the initial geometry which is presented in Table 1. We explicitly computed the number of these functions for several small values of k and used these results to formulate a conjecture for the general case.

Note that for the domain (d) we obtain (independently of k) only 3 such functions. The existence of at least 3 functions are guaranteed, since the constant function and the two (additional) linear functions on the computational domain are always contained in the space V. For the instances (a)-(c) the number $\nu(k)$ linearly increases with respect to k, which provides us a possibility to generate a sequence of nested spaces of C^1-smooth geometrically continuous isogeometric functions by refining the geometry mappings in an appropriate way (see Subsection 4.1). $\Diamond$

4. Numerical results

In this section we will consider the first nontrivial case, i.e., two-patch domains with C^1-continuous test functions over them. For different two-patch domains we will construct sequences of nested spaces of C^1-smooth geometrically continuous isogeometric functions by using bicubic and biquartic graphs of isogeometric elements. We will use these resulting functions to solve different partial differential equations, including L^2 approximation, solving the Poisson's equation and solving the biharmonic equation.

4.1. Setting of two-patch configurations

We consider again the case of a two-patch domain Ω, consisting of two patches $\Omega^{(1)}$ and $\Omega^{(2)}$, i.e. $\Omega = \Omega^{(1)} \cup \Omega^{(2)}$, which are glued together in such a way that they share the whole common edge (see e.g. Figure 2 and 3). We will construct a sequence of nested spaces of C^1-smooth geometrically continuous isogeometric functions defined on this two-patch domain Ω.

More precisely, we consider the case of two bilinear patches without any further symmetries (similar to case (c) in Figure 2), which are represented as bicubic ($p = 3$) or biquartic ($p = 4$) patches using degree elevation. In addition, in order to obtain a finer space, we insert $2^L - 1$, $L \in \mathbb{N}$, equidistant inner knots of multiplicity $p - 1$ in both parameter directions, where L is the *level of the refinement*. Moreover we also modified some of the control points (sufficiently far away from the interface) to obtain more general geometries.

By solving the linear system (6), we obtain C^1-smooth geometrically continuous isogeometric basis functions for a refined space, which will be denote by V_h, where $h = \mathcal{O}(2^{-L})$. The geometrically continuous isogeometric functions are globally C^1-smooth and piecewise C^∞-smooth, and therefore belong to the space $H^2(\Omega)$. Since all functions $v' \in V_{h'}$ can be represented as linear combinations of functions $v \in V_h$ for $h \leq h'$, we get a sequence of nested spaces $V_h \subset H^2(\Omega)$.

Later, for solving the Poisson's equation and the biharmonic equation, respectively, we will need C^1-smooth geometrically continuous isogeometric functions w_i, which satisfy the boundary conditions

$$w_i(\boldsymbol{x}) = 0 \text{ on } \partial\Omega$$

and

$$w_i(\boldsymbol{x}) = \frac{\partial w_i}{\partial \boldsymbol{n}}(\boldsymbol{x}) = 0 \text{ on } \partial\Omega,$$

respectively. We obtain sequences of nested spaces by solving the linear system (6) with additional linear equations for the corresponding boundary conditions. These spaces will be denoted by $V_{0,0h}$ and $V_{1,0h}$, respectively. In case of the Poisson's equation we get

$$V_{0,0h} \subset H_0^1(\Omega) = \{v \in H^1(\Omega) : v = 0 \text{ on } \partial\Omega\},$$

(more precisely, $V_{0,0h} \subset H_0^1(\Omega) \cap H^2(\Omega)$), and in case of the biharmonic equation we obtain

$$V_{1,0h} \subset H_0^2(\Omega) = \{v \in H^2(\Omega) : v = \frac{\partial v}{\partial \boldsymbol{n}} = 0 \text{ on } \partial\Omega\}.$$

Example 4. We consider the three different computational domains Ω, shown in Figure 3 (first row), which consist of two quadrilateral patches $\Omega^{(1)}$ and $\Omega^{(2)}$. For the domains (a) and (b), the corresponding initial geometry mappings $\boldsymbol{G}^{(1)}$ and $\boldsymbol{G}^{(2)}$ are bilinear parameterizations, which are represented as Bézier patches of degree (p, p) for $p = 3, 4$. In case of domain (c), the initial geometry mappings $\boldsymbol{G}^{(1)}$ and $\boldsymbol{G}^{(2)}$ are again Bézier patches of degree (p, p) for $p = 3, 4$, but they are chosen in such a way that the control points of the common edge and of the first neighboring columns are a part of a bilinear parameterization. In addition, the figure also shows the different exact analytic solutions, which will be used in the remaining examples in this section to verify the order of convergence.

Table 2 reports the number of isogeometric basis functions for various levels L of refinement and for the different boundary conditions. $\Diamond$

In the following subsections we present three possible applications of these isogeometric functions over two-patch domains, in order to demonstrate their potential for IgA on the basis of several examples.

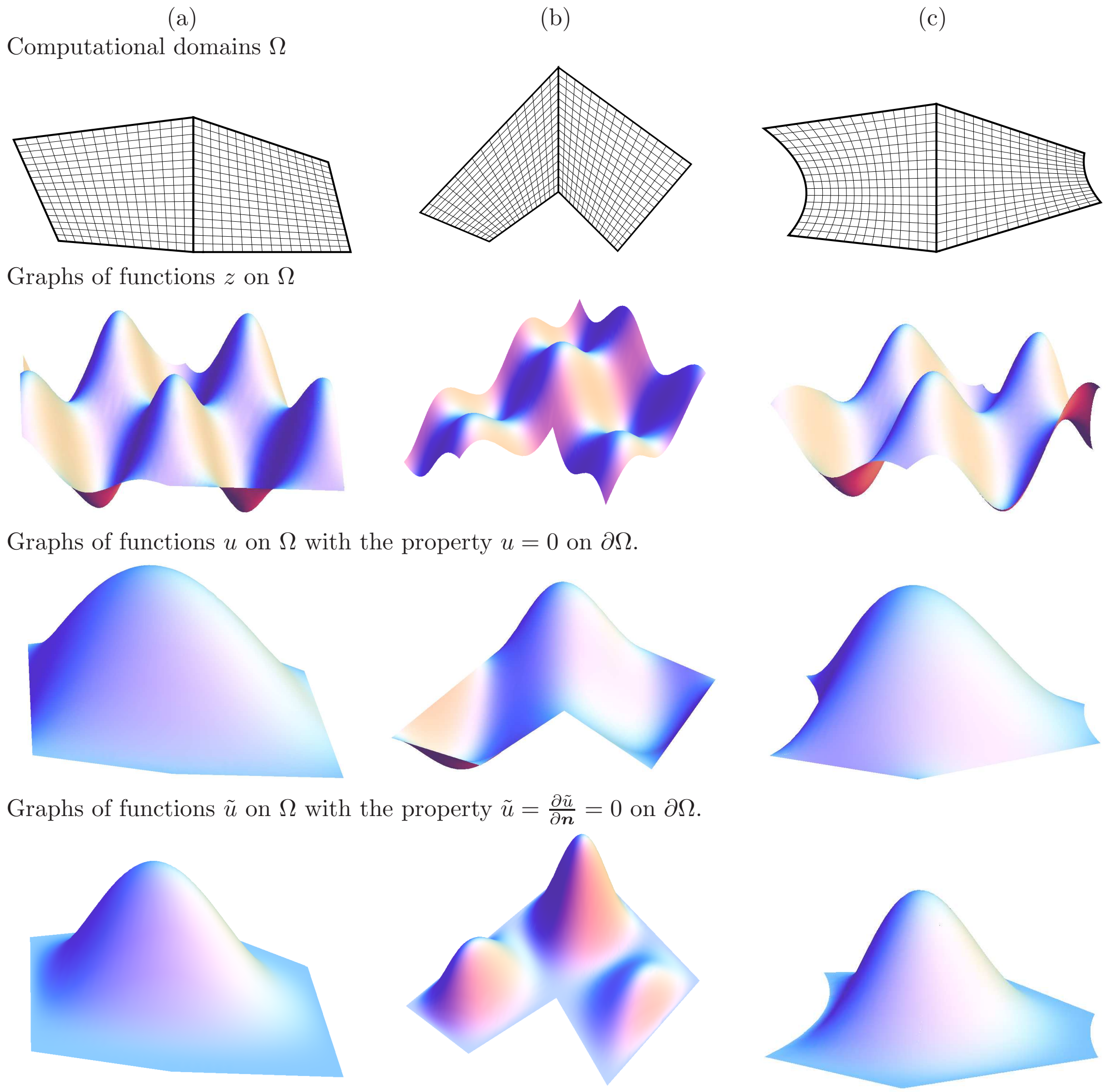

Figure 3: Three different two-patch domains Ω (first row) on which different functions are defined, which are to be approximated by L^2 norm minimization (second row) in Example 5, or used as exact solutions (third row) for Poisson's equation in Example 6, or as exact solutions (fourth row) for the biharmonic equation in Example 7.

4.2. L^2 approximation

Let $z : \Omega \to \mathbb{R}$ be a smooth function defined on a two-patch domain $\Omega = \Omega^{(1)} \cup \Omega^{(2)}$. In addition, let $\{w_i\}_{i \in I}$ for $I = \{1, 2, \ldots \dim V_h\}$ be a set of C^1-smooth geometrically continuous isogeometric functions, which form a basis of a subspace V_h of $H^2(\Omega)$. We approximate the function z by the function

$$u_h(\boldsymbol{x}) = \sum_{i \in I} c_i w_i(\boldsymbol{x}), \quad c_i \in \mathbb{R},$$

b.c.		L^2 approximation				Poisson's equation				Biharmonic equation			
		Bicubic		Biquartic		Bicubic		Biquartic		Bicubic		Biquartic	
L	# patches	# bfct	# k2	# bfct	# k2	# bfct	# k2	# bfct	# k2	# bfct	# k2	# bfct	# k2
0	2	23	7	39	9	5	1	15	3	-		-	
1	8	57	9	109	13	27	3	67	7	-		35	3
2	32	173	13	357	21	119	7	279	15	75	3	211	11
3	128	597	21	1285	37	495	15	1135	31	403	11	995	27
4	512	2213	37	4869	69	2015	31	4575	63	1827	27	4291	59
5	2048	8517	69	19849	133	8127	63	18367	127	7747	59	17795	123

Table 2: The number of C^1-smooth geometrically continuous isogeometric basis functions (# bfct: in total, # k2: second kind) for each level L for the three domains in Fig. 7 without boundary conditions (for L^2 approximation) and with homogeneous boundary conditions of order 0 and 1 (for Poisson's equation and for the biharmonic equation).

using the least squares approach, i.e., we compute the coefficients $\{c_i\}_{i\in I}$ such that

$$\|u_h - z\|_0^2 = \int_\Omega (u_h(\boldsymbol{x}) - z(\boldsymbol{x}))^2 \mathrm{d}\boldsymbol{x} \to \min_{c_i,\, i\in I} . \tag{10}$$

The minimization problem (10) can be formulated as a system of linear equations $K\boldsymbol{c} = \boldsymbol{z}$ for the unknown coefficients $\boldsymbol{c} = (c_i)_{i\in I}$, where the elements of the (mass) matrix $K = (k_{i,j})_{i,j\in I}$ and of the vector $\boldsymbol{z} = (z_i)_{i\in I}$ are

$$k_{i,j} = \int_\Omega w_i(\boldsymbol{x}) w_j(\boldsymbol{x}) \mathrm{d}\boldsymbol{x} \quad \text{and} \quad z_i = \int_\Omega z(\boldsymbol{x}) w_i(\boldsymbol{x}) \mathrm{d}\boldsymbol{x}.$$

Since the functions w_i are given as in (1) the entries $k_{i,j}$ and z_i can be rewritten as

$$k_{i,j} = k_{i,j}^{(1)} + k_{i,j}^{(2)}, \quad k_{i,j}^{(\ell)} = \int_{[0,1]^2} \omega_i^{(\ell)}(\boldsymbol{\xi}^{(\ell)})\, \omega_j^{(\ell)}(\boldsymbol{\xi}^{(\ell)}) |\det J^{(\ell)}(\boldsymbol{\xi}^{(\ell)})| \,\mathrm{d}\boldsymbol{\xi}^{(\ell)}, \quad \ell = 1, 2,$$

and

$$z_i = z_i^{(1)} + z_i^{(2)}, \quad z_{i,j}^{(\ell)} = \int_{[0,1]^2} z(\boldsymbol{G}^{(\ell)}(\boldsymbol{\xi}^{(\ell)}))\, \omega_i^{(\ell)}(\boldsymbol{\xi}^{(\ell)}) |\det J^{(\ell)}(\boldsymbol{\xi}^{(\ell)})| \,\mathrm{d}\boldsymbol{\xi}^{(\ell)}, \quad \ell = 1, 2,$$

where $J^{(\ell)}$ is the Jacobian of $\boldsymbol{G}^{(\ell)}$.

Example 5. We use the isogeometric basis functions on the three domains described in the previous example to apply L^2 approximation to smooth functions, which are defined on the domains (a)-(c).

More precisely, we approximate for all three domains the same function

$$z(x_1, x_2) = 2\cos(2x_1)\sin(2x_2), \tag{11}$$

restricted to the different domains, see Figure 3 (second row). The resulting H^0-errors (i.e. L^2-errors) and convergence rates for the different level L of refinement are presented in Table 3. The numerical results indicate that the convergence rate is optimal with respect to the H^0-norm, which is $\mathcal{O}(h^4)$ and $\mathcal{O}(h^5)$ for bicubic and biquartic cases, respectively. $\Diamond$

	Bicubic						Biquartic					
	Domain (a)		Domain (b)		Domain (c)		Domain (a)		Domain (b)		Domain (c)	
L	$\frac{\|\|z-u_h\|\|_0}{\|\|z\|\|_0}$	c.r. $\|\|\cdot\|\|_0$	$\frac{\|\|z-u_h\|\|_0}{\|\|z\|\|_0}$	c.r. $\|\|\cdot\|\|_0$	$\frac{\|\|z-u_h\|\|_0}{\|\|z\|\|_0}$	c.r. $\|\|\cdot\|\|_0$	$\frac{\|\|z-u_h\|\|_0}{\|\|z\|\|_0}$	c.r. $\|\|\cdot\|\|_0$	$\frac{\|\|z-u_h\|\|_0}{\|\|z\|\|_0}$	c.r. $\|\|\cdot\|\|_0$	$\frac{\|\|z-u_h\|\|_0}{\|\|z\|\|_0}$	c.r. $\|\|\cdot\|\|_0$
0	0.62276	-	0.60175	-	0.44238	-	0.09259	-	0.36954	-	0.09068	-
1	0.05315	3.5505	0.18912	1.67	0.04593	3.2679	0.0157	2.5603	0.03667	3.333	0.00987	3.1992
2	0.00614	3.114	0.01192	3.9879	0.0054	3.0917	0.00042	5.235	0.00272	3.7524	0.00031	4.9781
3	0.0005	3.6293	0.00126	3.2469	0.00038	3.8381	$9.6\ 10^{-6}$	5.438	0.00005	5.6651	$8.3\ 10^{-6}$	5.2331
4	0.00004	3.7407	0.0001	3.5831	0.00003	3.7617	$2.6\ 10^{-7}$	5.2044	$1.3\ 10^{-6}$	5.3824	$2.3\ 10^{-7}$	5.1522
5	$2.5\ 10^{-6}$	3.9087	$7.4\ 10^{-6}$	3.8275	$1.9\ 10^{-6}$	3.8892	$7.5\ 10^{-9}$	5.1122	$3.6\ 10^{-8}$	5.1611	$6.7\ 10^{-9}$	5.1263

Table 3: The relative H^0-errors with the estimated convergence rates (c.r.; the dyadic logarithm of the ratio of two consecutive relative errors) obtained by approximating the function z, defined in (11), using L^2 norm minimization (see Example 5 and Figure 3, first and second row).

4.3. Poisson's equation

We consider again a two–patch domain $\Omega = \Omega^{(1)} \cup \Omega^{(2)}$, and a set $\{w_i\}_{i\in I}$ for $I = \{1, 2, \ldots \dim V_{0,0h}\}$ of C^1-smooth geometrically continuous isogeometric functions, which form a basis of a subspace $V_{0,0h} \subset H_0^1(\Omega)$. We consider the following problem for the unknown function u over the computational domain Ω,

$$\begin{cases} \triangle u(\boldsymbol{x}) &= f(\boldsymbol{x}) \quad \text{on } \Omega \\ \quad u(\boldsymbol{x}) &= 0 \qquad\ \ \text{on } \partial\Omega \end{cases} \tag{12}$$

with $f \in H^0(\Omega)$. Using the weak formulation and a applying isogeometric Galerkin projection (cf. [6]) leads to a system of linear equations

$$S\boldsymbol{c} = \boldsymbol{f}$$

for the unknown coefficients $\boldsymbol{c} = (c_i)_{i\in I}$, where the entries of the stiffness matrix $S = (s_{i,j})_{i,j\in I}$ and of the load vector $\boldsymbol{f} = (f_i)_{i\in I}$ are given by

$$s_{i,j} = \int_\Omega (\nabla w_i(\boldsymbol{x}))^T \nabla w_j(\boldsymbol{x}) \mathrm{d}\boldsymbol{x} \quad \text{and} \quad f_i = \int_\Omega f(\boldsymbol{x}) w_i(\boldsymbol{x}) \mathrm{d}\boldsymbol{x}, \tag{13}$$

respectively. Using the isogeometric approach, we rewrite these integrals as

$$s_{i,j} = s_{i,j}^{(1)} + s_{i,j}^{(2)}, \quad s_{i,j}^{(\ell)} = \int_{[0,1]^2} (\nabla \omega_i^{(\ell)}(\boldsymbol{\xi}^{(\ell)}))^T N^{(\ell)}(\boldsymbol{\xi}^{(\ell)}) \nabla \omega_j^{(\ell)}(\boldsymbol{\xi}^{(\ell)})\, \mathrm{d}\boldsymbol{\xi}^{(\ell)}, \quad \ell = 1, 2,$$

and

$$f_i = f_i^{(1)} + f_i^{(2)}, \quad f_{i,j}^{(\ell)} = \int_{[0,1]^2} f(\boldsymbol{G}^{(\ell)}(\boldsymbol{\xi}^{(\ell)})) \omega_i^{(\ell)}(\boldsymbol{\xi}^{(\ell)}) |\det J^{(\ell)}(\boldsymbol{\xi}^{(\ell)})|\, \mathrm{d}\boldsymbol{\xi}^{(\ell)}, \quad \ell = 1, 2,$$

with

$$N^{(\ell)}(\boldsymbol{\xi}^{(\ell)}) = \left(J^{(\ell)}(\boldsymbol{\xi}^{(\ell)})\right)^{-T} \left(J^{(\ell)}(\boldsymbol{\xi}^{(\ell)})\right)^{-1} |\det J^{(\ell)}(\boldsymbol{\xi}^{(\ell)})|, \quad \ell = 1, 2.$$

	Domain (a)				Domain (b)				Domain (c)			
	$\frac{\|\|u-u_h\|\|_0}{\|\|u\|\|_0}$	c.r. $\|\|\cdot\|\|_0$	$\frac{\|\|u-u_h\|\|_1}{\|\|u\|\|_1}$	c.r. $\|\|\cdot\|\|_1$	$\frac{\|\|u-u_h\|\|_0}{\|\|u\|\|_0}$	c.r. $\|\|\cdot\|\|_0$	$\frac{\|\|u-u_h\|\|_1}{\|\|u\|\|_1}$	c.r. $\|\|\cdot\|\|_1$	$\frac{\|\|u-u_h\|\|_0}{\|\|u\|\|_0}$	c.r. $\|\|\cdot\|\|_0$	$\frac{\|\|u-u_h\|\|_1}{\|\|u\|\|_1}$	c.r. $\|\|\cdot\|\|_1$
L	Bicubic											
0	0.76824	-	0.79715	-	0.85307	-	0.78634	-	0.77419	-	0.79388	-
1	0.0312	4.6219	0.06712	3.5701	0.15608	2.4504	0.21366	1.8798	0.08635	3.1645	0.16776	2.2425
2	0.00145	4.4272	0.00762	3.1382	0.0053	4.88	0.01752	3.6084	0.01184	2.867	0.03805	2.1406
3	0.00009	4.0313	0.00097	2.9709	0.00021	4.625	0.00177	3.3082	0.00055	4.4407	0.00402	3.2438
4	$5.7\ 10^{-6}$	3.9702	0.00012	2.9675	0.00001	4.2529	0.00021	3.0843	0.00003	4.4278	0.00048	3.0505
5	$3.6\ 10^{-7}$	3.9765	0.00002	2.981	$6.8\ 10^{-7}$	4.0479	0.00003	3.014	$1.5\ 10^{-6}$	4.0772	0.00006	2.9304
L	Biquartic											
0	0.01303	-	0.0256	-	0.16407	-	0.20565	-	0.06356	-	0.10765	-
1	0.00059	4.4648	0.00207	3.6269	0.0064	4.6792	0.01542	3.7376	0.01069	2.5717	0.03546	1.6022
2	0.00002	4.8915	0.00013	3.9454	0.0002	5.0164	0.00094	4.0393	0.00055	4.2792	0.00341	3.3765
3	$5.6\ 10^{-7}$	5.1539	$7.8\ 10^{-6}$	4.1024	$5.3\ 10^{-6}$	5.2141	0.00005	4.2045	0.00002	4.9272	0.00023	3.9074
4	$1.4\ 10^{-8}$	5.3021	$4.3\ 10^{-7}$	4.18	$1.3\ 10^{-7}$	5.3376	$2.6\ 10^{-6}$	4.2651	$5\ 10^{-7}$	5.1786	0.00001	4.0898
5	$3.5\ 10^{-10}$	5.3383	$2.4\ 10^{-8}$	4.1744	$3.2\ 10^{-9}$	5.3586	$1.4\ 10^{-7}$	4.2482	$1.3\ 10^{-8}$	5.2902	$7.5\ 10^{-7}$	4.1526

Table 4: The relative H^i-errors, $i = 0, 1$, with the corresponding estimated convergence rates (c.r.: the dyadic logarithm of the ratio of two consecutive relative errors) obtained by solving the Poisson's equations for different exact solutions u, for the domains (a)-(c) (see Example 6 and Figure 3, first and third row).

Example 6. We consider again the three computational domains, which are shown in Figure 3 (first row). For each of the domains (a)-(c) we consider a different right side function f of the Poisson's equation (12), which are obtained by differentiating

$$u_a(x_1, x_2) = 10^{-\frac{5}{2}} x_2\big(\tfrac{1}{12}x_1 + x_2\big)(4x_1 + x_2 - 14)\big(\tfrac{1}{3}x_1 + x_2 - 3\big)\big(\tfrac{1}{8}x_1 - x_2 + 3\big)\big(\tfrac{9}{4}x_1 + x_2 + \tfrac{13}{2}\big),$$

$$\begin{aligned} u_b(x_1, x_2) = \;& \tfrac{1}{20\sqrt{10}}\left(\tfrac{18}{25}x_1 - x_2\right)(x_1 + x_2)\left(3 + \tfrac{21}{20}x_1 - x_2\right)\left(3 - \tfrac{25}{48}x_1 - x_2\right) \\ & \left(\tfrac{19}{10} + \tfrac{21}{50}x_1 + x_2\right)\left(\tfrac{290}{93} - \tfrac{110}{93}x_1 + x_2\right), \end{aligned}$$

and

$$\begin{aligned} u_c(x_1, x_2) = \;& \tfrac{1}{100\sqrt{2}}\left(2\left(\tfrac{128327}{48672} + x_1\right) + \left(x_2 - \tfrac{185}{156}\right)^2\right)\left(2\left(\tfrac{215}{72} - x_1\right) + \left(x_2 - \tfrac{11}{6}\right)^2\right) \\ & \left(\tfrac{1}{9}x_1 + x_2\right)\left(\tfrac{3}{10}x_1 - x_2\right)\left(3 + \tfrac{1}{7}x_1 - x_2\right)\left(3 - \tfrac{1}{3}x_1 - x_2\right), \end{aligned}$$

respectively. The three functions satisfy the boundary conditions $u = 0$ on $\partial\Omega$, and are visualized in Figure 3 (third row). The resulting H^i-errors, $i = 0, 1$, with the corresponding convergence rates are presented in Table 4. The numerical results indicate convergence rates of $\mathcal{O}(h^{4-i})$ and $\mathcal{O}(h^{5-i})$ in the H^i-norms, $i = 0, 1$, for the bicubic and the biquartic case, respectively. $\Diamond$

4.4. Biharmonic equation

Higher order smoothness of isogeometric elements is particularly advantageous for solving high order partial differential equations. An example of such an equation is (the weak formulation of) the biharmonic equation, where C^1 smoothness of isogeometric functions is an advantage, since test functions from the space $H^2(\Omega)$ are required (cf. [5, 18]).

Let $\{w_i\}_{i \in I}$ for $I = \{1, 2, \ldots \dim V_{1,0h}\}$ be a set of C^1-smooth geometrically continuous isogeometric functions, which form a basis of a subspace $V_{1,0h}$ of $H^2_0(\Omega)$, where $\Omega = \Omega^{(1)} \cup$

$\Omega^{(2)}$ is a two-patch domain. As a model problem we consider the first biharmonic boundary value problem for the unknown function u over the computational domain Ω,

$$\left\{ \begin{array}{rll} \triangle^2 u(\boldsymbol{x}) & = f(\boldsymbol{x}) & \text{on } \Omega \\ u(\boldsymbol{x}) = \frac{\partial u}{\partial \boldsymbol{n}}(\boldsymbol{x}) & = 0 & \text{on } \partial\Omega \end{array} \right. , \tag{14}$$

with $f \in H^0(\Omega)$. Using the weak formulation, we compute $u \in H_0^2(\Omega)$ such that

$$\int_\Omega \triangle u(\boldsymbol{x}) \triangle v(\boldsymbol{x}) \mathrm{d}\boldsymbol{x} = \int_\Omega f(\boldsymbol{x}) v(\boldsymbol{x}) \mathrm{d}\boldsymbol{x}$$

for all $v \in H_0^2(\Omega)$ (see [18]). Using the Galerkin projection we find $v_h \in V_{1,0h}$ by solving the system of equations

$$\int_\Omega \triangle u_h(\boldsymbol{x}) \triangle v_h(\boldsymbol{x}) \mathrm{d}\boldsymbol{x} = \int_\Omega f(\boldsymbol{x}) v_h(\boldsymbol{x}) \mathrm{d}\boldsymbol{x}$$

for all $v_h \in V_{1,0h}$, which leads to a system of linear equations. More precisely, we are solving the linear system $S\boldsymbol{c} = \boldsymbol{f}$, for the coefficients of

$$u_h(\boldsymbol{x}) = \sum_{i \in I} c_i w_i(\boldsymbol{x}),$$

where

$$s_{i,j} = \int_\Omega \triangle w_i(\boldsymbol{x}) \triangle w_j(\boldsymbol{x}) \mathrm{d}\boldsymbol{x} \quad \text{and} \quad f_i = \int_\Omega f(\boldsymbol{x}) w_i(\boldsymbol{x}) \, \mathrm{d}\boldsymbol{x},$$

respectively. After some computations we arrive at the following formulas for the elements of the stiffness matrix and the load vector for the two-patch isogeometric case:

$$s_{i,j} = s_{i,j}^{(1)} + s_{i,j}^{(2)}, \quad s_{i,j}^{(\ell)} = \int_{[0,1]^2} \operatorname{tr}\left(\widetilde{M}_i^{(\ell)}(\boldsymbol{\xi}^{(\ell)})\right) \operatorname{tr}\left(\widetilde{M}_j^{(\ell)}(\boldsymbol{\xi}^{(\ell)})\right) \frac{1}{|\det J^{(\ell)}(\boldsymbol{\xi}^{(\ell)})|} \, \mathrm{d}\boldsymbol{\xi}^{(\ell)}, \quad \ell = 1, 2,$$

and

$$f_i = f_i^{(1)} + f_i^{(2)}, \quad f_{i,j}^{(\ell)} = \int_{[0,1]^2} f(\boldsymbol{G}^{(\ell)}(\boldsymbol{\xi}^{(\ell)})) \omega_i^{(\ell)}(\boldsymbol{\xi}^{(\ell)}) |\det J^{(\ell)}(\boldsymbol{\xi}^{(\ell)})| \, \mathrm{d}\boldsymbol{\xi}^{(\ell)}, \quad \ell = 1, 2,$$

with

$$\widetilde{M}_i^{(\ell)}(\boldsymbol{\xi}^{(\ell)}) = \left(J^{(\ell)}(\boldsymbol{\xi}^{(\ell)})\right)^{-T} M_i^{(\ell)}(\boldsymbol{\xi}^{(\ell)}) \left(J^{(\ell)}(\boldsymbol{\xi}^{(\ell)})\right)^{-1},$$

where $M_i^{(\ell)} = \left(m_{i;r,s}^{(\ell)}\right)_{r,s=1,2}$ is given by

$$m_{i;r,s}^{(\ell)} = \left(\frac{\partial^2 \boldsymbol{F}_i^{(\ell)}}{\partial \xi_r^{(\ell)} \partial \xi_s^{(\ell)}} (\boldsymbol{\xi}^{(\ell)}))^T \cdot \left(\frac{\partial \boldsymbol{F}_i^{(\ell)}}{\partial \xi_1^{(\ell)}} (\boldsymbol{\xi}^{(\ell)}) \times \frac{\partial \boldsymbol{F}_i^{(\ell)}}{\partial \xi_2^{(\ell)}} (\boldsymbol{\xi}^{(\ell)}) \right) \right).$$

	Bicubic						Biquartic					
	$\frac{\|\|u-u_h\|\|_0}{\|\|u\|\|_0}$	c.r. $\|\|\cdot\|\|_0$	$\frac{\|\|u-u_h\|\|_1}{\|\|u\|\|_1}$	c.r. $\|\|\cdot\|\|_1$	$\frac{\|\|u-u_h\|\|_2}{\|\|u\|\|_2}$	c.r. $\|\|\cdot\|\|_2$	$\frac{\|\|u-u_h\|\|_0}{\|\|u\|\|_0}$	c.r. $\|\|\cdot\|\|_0$	$\frac{\|\|u-u_h\|\|_1}{\|\|u\|\|_1}$	c.r. $\|\|\cdot\|\|_1$	$\frac{\|\|u-u_h\|\|_2}{\|\|u\|\|_2}$	c.r. $\|\|\cdot\|\|_2$
L	Domain (a)											
1	-	-	-	-	-	-	0.03487	-	0.0825	-	0.21691	-
2	0.0854	-	0.10026	-	0.19868	-	0.01122	1.6367	0.01529	2.4316	0.04748	2.1916
3	0.01023	3.0619	0.01322	2.9231	0.04907	2.0175	0.00068	4.0498	0.00118	3.6939	0.0077	2.6253
4	0.00099	3.3717	0.00147	3.1638	0.01207	2.0237	0.00003	4.6554	0.00006	4.2169	0.00095	3.0169
5	0.00007	3.9088	0.00013	3.5344	0.00286	2.0758	$8.8\ 10^{-7}$	4.9244	$3.2\ 10^{-6}$	4.3237	0.00011	3.0704
L	Domain (b)											
1	-	-	-	-	-	-	0.28053	-	0.36533	-	0.45296	-
2	0.26249	-	0.35642	-	0.46964	-	0.0067	5.3871	0.0182	4.327	0.05738	2.9808
3	0.00751	5.1264	0.01511	4.5602	0.07582	2.6309	0.00059	3.6641	0.00235	2.9509	0.01407	2.0271
4	0.0007	3.4276	0.00252	2.5817	0.0214	1.825	0.00002	4.9899	0.00015	3.935	0.00187	2.9112
5	0.00004	4.0957	0.00026	3.3062	0.00514	2.0572	$3.7\ 10^{-7}$	5.4819	$7.9\ 10^{-6}$	4.2917	0.0002	3.206
L	Domain (c)											
1	-	-	-	-	-	-	0.15127	-	0.19195	-	0.34591	-
2	0.23492	-	0.26927	-	0.39737	-	0.00435	5.12	0.01153	4.0569	0.06199	2.4803
3	0.0037	5.9883	0.00827	5.0256	0.06516	2.6084	0.00141	1.6242	0.00273	2.0813	0.01605	1.9491
4	0.00149	1.3077	0.00266	1.637	0.01976	1.7218	0.00008	4.076	0.00022	3.6083	0.00284	2.499
5	0.00014	3.4688	0.0003	3.1319	0.00491	2.0072	$3.2\ 10^{-6}$	4.7036	0.00001	4.1635	0.00036	2.9718

Table 5: The relative H^i-errors, $i = 0, 1, 2$, with the corresponding estimated convergence rates (c.r.; the dyadic logarithm of the ratio of two consecutive relative errors) obtained by solving the biharmonic equations for different exact solutions $\tilde{u}$, for the domains (a)-(c) (see Example 7 and Figure 3, first and fourth row).

Example 7. We numerically solve the biharmonic equation (14) over the same three computational domains Ω with the same associated initial geometry mappings $\boldsymbol{G}^{(1)}$ and $\boldsymbol{G}^{(2)}$ as in Example 5 and 6 (see Figure 3, first row). We use the nested spaces $V_{1,0h} \subset H_0^2(\Omega)$ of C^1-smooth geometrically continuous isogeometric functions for degree $p = 3, 4$, where the number of resulting functions (for each level L) are presented in Table 2. Note, that for the bicubic and the biquartic case, there do not exist non-trivial geometrically continuous isogeometric functions for low levels L, due to the boundary conditions. Therefore, the coarsest level starts with $L = 2$ and $L = 1$ for $p = 3$ and $p = 4$, respectively.

The right-hand side functions f of the biharmonic equation (14) for the domains (a)-(c) are obtained by differentiating the functions $\tilde{u} = u^2$, where u are the corresponding functions from Example 6. These functions fulfill the boundary conditions $\tilde{u} = \frac{\partial \tilde{u}}{\partial \boldsymbol{n}} = 0$ on $\partial\Omega$, and are visualized in Figure 3 (fourth row). The resulting H^i-errors, $i = 0, 1, 2$, with the corresponding convergence rates are presented in Table 5. For the the numerical results indicate a convergence rate $\mathcal{O}(h^2)$ and $\mathcal{O}(h^3)$ for the bicubic and the biquartic case, respectively. $\Diamond$

5. Conclusion

We discussed C^s-smooth geometrically continuous isogeometric functions defined on multi-patch domains $\Omega \subset \mathbb{R}^2$. Their construction is based on the observation that the geometric smoothness of the graph of such a function is equivalent to the smoothness of the function over Ω. We also sketched a procedure to construct a basis for the space of C^s-smooth geometrically continuous isogeometric functions.

The potential of the resulting geometrically continuous isogeometric functions has been demonstrated by several examples, including L^2 approximation, the Poisson's equation and the biharmonic equation. For these examples, we considered different two patch-domains Ω consisting of two quadrilateral patches, for which we generated geometrically continuous isogeometric functions of order 1 and degree $p = 3, 4$. For all three different applications, the numerical results indicated optimal convergence rates.

This is different from the experiments reported in [11], where a reduction of the order of convergence for geometrically continuous discretizations has been observed. A possible explanation is the fact that the effect of geometric continuity in those experiments was concentrated at an extraordinary vertex, while we spread it out along the entire interface between two patches. In fact, many constructions for geometrically continuous surfaces in geometric modeling aim at limiting the effect of geometric continuity to the vicinity of extraordinary vertices [13], as it is then possible to use standard constructions everywhere except at very few places. However, our experiments seem to indicate that spreading out the effect to geometric continuity is more appropriate for applications in isogeometric analysis, in order to maintain the approximation power. Moreover, the latter approach makes it also simpler to obtain nested spaces by h-refinement.

The present paper is restricted to two-patch domains. In order to overcome this limitation, we are currently working on using our general framework to generate C^1 smooth geometrically continuous isogeometric functions for multi-patch domains with extraordinary vertices. A detailed investigation of the structure of the resulting spaces of geometrically continuous isogeometric functions is of interest, too. On the one hand we could generate basis functions with a small support, if feasible. On the other hand we aim at finding explicit formulae, depending on the initial geometry, for the coefficients of the isogeometric functions.

Another possible topic of future work is a theoretical investigation of experimentally obtained approximation power of the geometrically continuous isogeometric functions. Moreover, one may use the considered class of two-patch domains as a reference configuration to construct geometrically continuous isogeometric functions for more general two-patch domains, such as domains without a line as common boundary. Finally, the extension of the concept of geometrically continuous isogeometric functions to three-dimensional multi-patch domains should be considered.

Acknowledgments. Supported by the Austrian Research Fund (FWF) through Grant NFN (National Research Network) S117 "Geometry +Simulation".

References

[1] Y. Bazilevs, V. M. Calo, J. A. Cottrell, J. A. Evans, T. J. R. Hughes, S. Lipton, M. A. Scott, and T. W. Sederberg. Isogeometric analysis using T-splines. *Comp. Methods Appl. Mech. Engrg.*, 199(5–8):229 – 263, 2010.

[2] L. Beirão da Veiga, A. Buffa, D. Cho, and G. Sangalli. IsoGeometric analysis using T-splines on two-patch geometries. *Comp. Methods Appl. Mech. Engrg.*, 200(21–22):1787 – 1803, 2011.

[3] L. Beirão da Veiga, A. Buffa, G. Sangalli, and R. Vázquez. Mathematical analysis of variational isogeometric methods. *Acta Numerica*, 23:157–287, 5 2014.

[4] D. Burkhart, B. Hamann, and G. Umlauf. Iso-geometric analysis based on Catmull-Clark solid subdivision. *Computer Graphics Forum*, 29(5):1575–1784, 2010.

[5] P. G. Ciarlet. *The Finite Element Method for Elliptic Problems*. Society for Industrial and Applied Mathematics, 2002.

[6] J. A. Cottrell, T.J.R. Hughes, and Y. Bazilevs. *Isogeometric Analysis: Toward Integration of CAD and FEA*. John Wiley & Sons, Chichester, England, 2009.

[7] J. Hoschek and D. Lasser. *Fundamentals of computer aided geometric design*. AK Peters Ltd., Wellesley, MA, 1993.

[8] T. J. R. Hughes, J. A. Cottrell, and Y. Bazilevs. Isogeometric analysis: CAD, finite elements, NURBS, exact geometry and mesh refinement. *Comput. Methods Appl. Mech. Engrg.*, 194(39-41):4135–4195, 2005.

[9] H.-J. Kim, Y.-D. Seo, and S.-K. Youn. Isogeometric analysis with trimming technique for problems of arbitrary complex topology. *Comp. Methods Appl. Mech. Engrg.*, 199(45–48):2796 – 2812, 2010.

[10] S. Kleiss, C. Pechstein, B. Jüttler, and S. Tomar. IETI – isogeometric tearing and interconnecting. *Comp. Methods Appl. Mech. Engrg.*, 247-248:201–215, 2012.

[11] T. Nguyen, K. Karčiauskas, and J. Peters. A comparative study of several classical, discrete differential and isogeometric methods for solving Poisson's equation on the disk. *Axioms*, 3(2):280–299, 2014.

[12] V.P. Nguyen, P. Kerfriden, M. Brino, S.P.A. Bordas, and E. Bonisoli. Nitsche's method for two and three dimensional NURBS patch coupling. *Comput. Mech.*, 53(6):1163–1182, 2014.

[13] J. Peters. Geometric continuity. In *Handbook of computer aided geometric design* (G. Farin, J. Hoschek and M.-S. Kim, eds.), pages 193–227. North-Holland, Amsterdam, 2002.

[14] J. Peters. Matched G^1-constructions yield C^1-continuous isogeometric elements. Technical Report 1406.4229, arXiv.org, 2014.

[15] J. Peters and U. Reif. *Subdivision surfaces*, volume 3 of *Geometry and Computing*. Springer-Verlag, Berlin, 2008.

[16] L. Piegl and W. Tiller. *The NURBS Book*. Springer, 1997.

[17] M. Ruess, D. Schillinger, A. I. Özcan, and E. Rank. Weak coupling for isogeometric analysis of non-matching and trimmed multi-patch geometries. *Comp. Methods Appl. Mech. Engrg.*, 269:46 – 71, 2014.

[18] S. Salsa. *Partial differential equations in action: From modelling to theory*. Universitext. Springer-Verlag Italia, Milan, 2008.

[19] R. Schmidt, R. Wüchner, and K.-U. Bletzinger. Isogeometric analysis of trimmed NURBS geometries. *Comp. Methods Appl. Mech. Engrg.*, 241–244:93–111, 2012.

[20] M. A. Scott, D. C. Thomas, and E. J. Evans. Isogeometric spline forests. *Comp. Methods Appl. Mech. Engrg.*, 269:222–264, 2014.

[21] T. W. Sederberg, G. T. Finnigan, X. Li, H. Lin, and H. Ipson. Watertight trimmed NURBS. *ACM Trans. Graphics*, 27(3), article no. 79, 2008.

[22] T. W. Sederberg, D. L. Cardon, G. T. Finnigan, N. S. North, J. Zheng, and T. Lyche. T-spline simplification and local refinement. *ACM Trans. Graph.*, 23(3):276–283, 2004.

[23] T. Takacs and B. Jüttler. Existence of stiffness matrix integrals for singularly parameterized domains in isogeometric analysis. *Comp. Methods Appl. Mech. Engrg.*, 200:3568–3582, 2011.

[24] X. Yuan and W. Ma. Mapped B-spline basis functions for shape design and isogeometric analysis over an arbitrary parameterization. *Comp. Methods Appl. Mech. Engrg.*, 269:87–107, 2014.